


Article

# Computational Analysis of the Automation Strategies of Temperatures of Supplied Air, Chilled and Condensation Water in Commercial Buildings

Javier Diaz-Valdivia and Flávio A. S. Fiorelli \* 

Polytechnic School, University of São Paulo, São Paulo 05508-010, Brazil

\* Correspondence: fiorelli@usp.br

**Abstract:** The automation strategies currently used in HVAC systems do not control the system temperature variables (supplied air, chilled, and condensation water temperatures) in an optimized way. Normally, these temperatures are fixed in design conditions, or vary according to the weather conditions. However, studies demonstrate that adequate control of these three temperatures can provide significant reductions in the energy consumption of the air conditioner system. Therefore, this work analyzes the benefits of individualized and integrated automation of these three variable temperatures in different tropical and subtropical weather conditions through computer simulation for a typical commercial building. The results of integrated automation show savings in consumption between 5.03% and 19.68% compared to a fixed control, and between 3.22% and 8.21% compared to a weather-based control alone, showing that the integrated strategies are better than both models adopted as market benchmarks.

**Keywords:** commercial building air conditioning; energy efficiency; control optimization; integrated strategies



**Citation:** Diaz-Valdivia, J.; Fiorelli, F.A.S. Computational Analysis of the Automation Strategies of Temperatures of Supplied Air, Chilled and Condensation Water in Commercial Buildings. *Energies* **2023**, *16*, 3445. <https://doi.org/10.3390/en16083445>

Academic Editors: Rafał Figaj and Mariusz Filipowicz

Received: 19 December 2022

Revised: 4 February 2023

Accepted: 7 February 2023

Published: 14 April 2023



**Copyright:** © 2023 by the authors. Licensee MDPI, Basel, Switzerland. This article is an open access article distributed under the terms and conditions of the Creative Commons Attribution (CC BY) license (<https://creativecommons.org/licenses/by/4.0/>).

## 1. Introduction

Energy consumption in buildings accounts for 32% of the global energy consumption [1], reaching 40% in Europe [2] and in the USA [3]. In Brazil, the commercial sector accounts for 15.7% of consumption [4]. Most of the consumption of a commercial building is due to the HVAC system, representing 50% of the building consumption in the USA [2], 76% in Europe [5] and 47% in Brazil [6]. Therefore, ways of reducing the consumption of this system must be investigated.

This work focuses on automation strategies in the chilled water plant of the HVAC system to reduce the building consumption. The HVAC system removes the thermal load from conditioned spaces by controlling three temperatures: supplied air temperature ( $T_{as}$ ); chilled water temperature at the outlet of the chiller ( $T_{chw}$ ); and water temperature at the outlet of the cooling tower ( $T_{ctw}$ ). This control acts by varying three flow rates: air supply flow; chilled water flow in the coil; and airflow in the cooling tower. Therefore, automation acts on these flow parameters and controls the temperatures ( $T_{as}$ ,  $T_{chw}$  and  $T_{ctw}$ ) as a function of the variation in the thermal load.

The simplest control strategy is to keep the three temperatures fixed to the design condition (worst-case scenario), following the RTQ-C, which is the Brazilian regulation on technical requirements and methods for classifying commercial buildings for energy efficiency [7]. This strategy is very inefficient since this situation occurs only 1% of the time and the system is oversized by 15% [8]. A more efficient strategy is to control the three temperatures as a function of outside weather conditions, following ASHRAE 90.1 [8]. However, this strategy is not optimized, as it does not consider variations in thermal load which is an important parameter according to [9].

Several studies in the literature show significant savings in HVAC consumption when optimized strategies of control are also based on thermal load variations. Using computational simulation, Ahn and Mitchell [10] show the possibility to obtain an optimum point for each one of three controllable temperatures in a specific condition. However, operational conditions change over time and this optimum point needs to be readjusted.

Albieri et al. [11] showed the possibility of reducing energy consumption with an isolated control of the  $T_{chw}$ . The authors developed an algorithm to control  $T_{chw}$  in a chiller with air condensation, which increased the seasonal efficiency of the chiller by 9.1%.

Concerning  $T_{as}$  optimal control, Wang and Song [12] obtained a reduction in HVAC consumption with this strategy, with higher values for lower outside temperatures and lower partial thermal loads. Similar behaviour was also observed by Ke and Mumma [13]: an annual reduction of 6.2% in Pennsylvania, with higher values in the spring and fall.

Finally, for the isolated control of the  $T_{ctw}$ , Braun and Diderrich [14] observed that there is an optimal point for the chiller-tower system. Additionally, Li et al. [3] showed a change in the optimal point change with the variation in the thermal load and weather conditions, indicating that  $T_{ctw}$  needs to be adjusted for each momentary condition. A similar behaviour was observed for Liu and Chuah [15], who obtained an annual energy consumption ranging from 4.1% to 5.9% for the chiller tower system.

By integrating two temperature controls, Parameshwaran et al. [16] simultaneously optimized  $T_{chw}$  and  $T_{as}$  and obtained a saving of 7.9% for an analysis of a dairy industry in India. Lee and Cheng [17] optimized the  $T_{chw}/T_{ctw}$  pair and obtained reductions of 9.4% in Taiwan in a summer week and 11.1% in a winter week.

The studies presented and others show that an optimized control of the aforementioned temperatures ( $T_{as}$ ,  $T_{chw}$ , and  $T_{ctw}$ ), both individually and combined in pairs, provide an optimization of energy consumption in air conditioning operation. In this sense, there is the possibility of increasing these gains with the full integration of the three temperature controls, and the possibility of analyzing such gains in tropical and subtropical weather conditions typical of countries such as Brazil, China, India, and others. Thus, by means of computational simulation, this study analyzes the impact of temperature control strategies (both isolated and integrated) in different Brazilian cities.

The results of this work indicate the benefits of both individualized and integrated automation of these three variable temperatures for a typical commercial building, by the reduction in energy consumption with a basically negligible cost in terms of return on investment since it involves the man-hour cost for reprogramming the control logic of existing systems and eventually a readjustment/repositioning of some sensors and actuators.

## 2. Materials and Methods

### 2.1. Building Parameters

For the present study, a building with 10 floors and a  $35 \times 35$  m quadratic plant is shown in Figures 1 and 2. The core and the elevator hall are located in the centre of the floor, and the office areas are located at the perimeter, which is maintained at  $24^\circ\text{C}$ . The floor has a height of 2.8 m plus a plenum of 1.15 m, totalling 3.95 m.

To analyze Brazilian weather, the Brazilian standard NBR 15220 [18] is used; it divides the country into eight bioclimatic zones with similar weather conditions, as shown in Figure 3. The study considered a representative city for each zone with its respective weather file to extrapolate the results for the entire Brazilian territory, as indicated in Table 1.

According to [8], the requirements for the building envelope for each bioclimatic zone (global heat transfer coefficient  $U$  and solar heat gain coefficient SHGC) are presented in Table 2, and a vertical glazing of 40% of the area of the walls is considered.

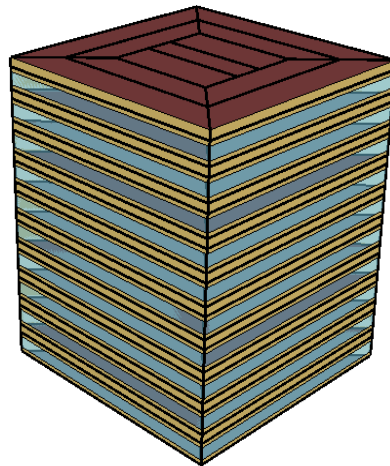


Figure 1. 3-D view of the considered building.

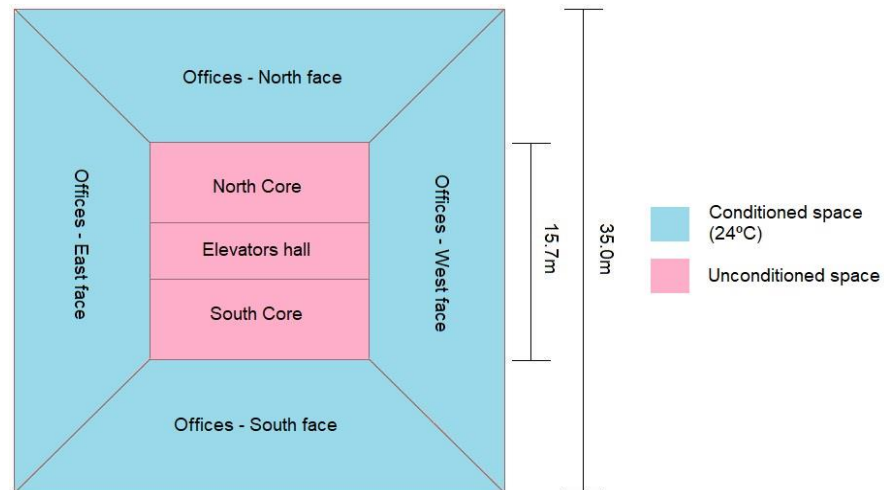


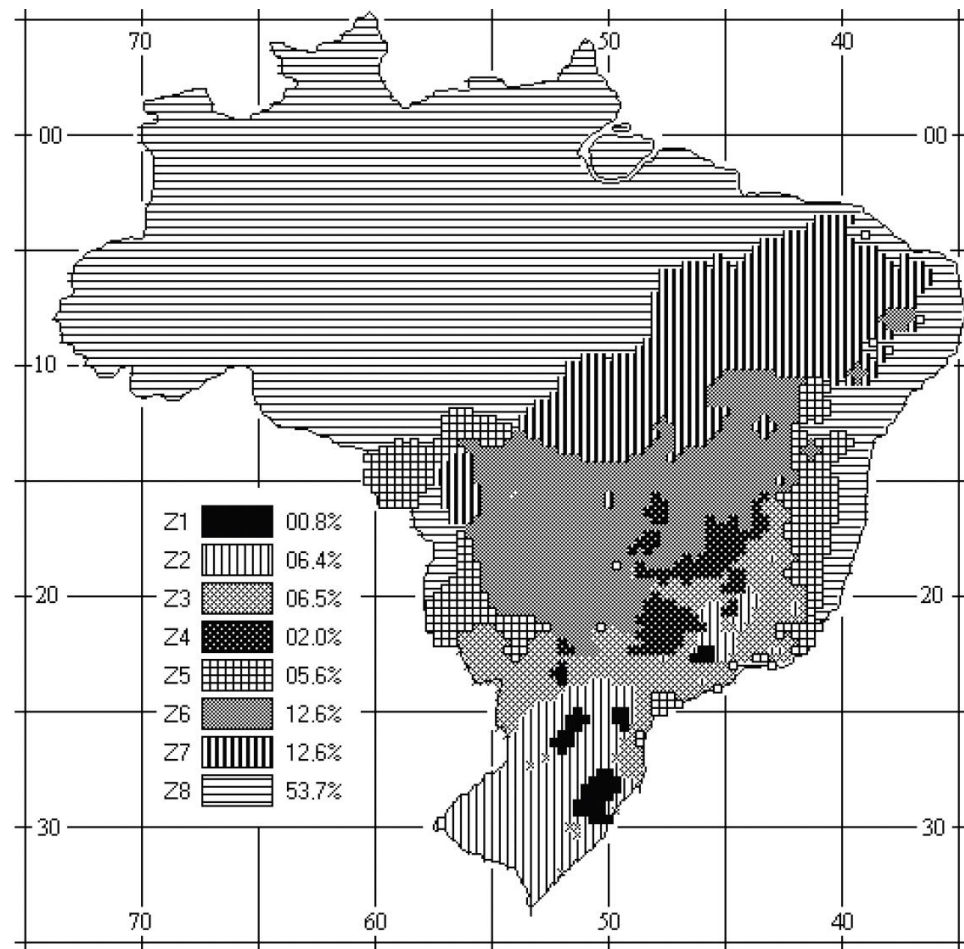
Figure 2. Building floor plan.

Table 1. Representative cities for the Brazilian bioclimatic zones [18,19].

Bioclimatic Zone	Representative City	Weather File
1	Curitiba	BRA_PR_Curitiba.838420_INMET.epw
2	Santa Maria	BRA_RS_Santa.Maria.839360_INMET.epw
3	São Paulo	BRA_SP_Sao.Paulo.837810_INMET.epw
4	Brasília	BRA_DF_Brasilia.867150_INMET.epw
5	Macaé	BRA_RJ_Macae.868910_INMET.epw
6	Goiânia	BRA_GO_Goiania.834230_INMET.epw
7	Teresina	BRA_PI_Teresina.818320_INMET.epw
8	Rio de Janeiro	BRA_RJ_Rio.de.Janeiro-Vila.Militar.868790_INMET.epw

Table 2. Values of U and SHGC for representative cities [8].

Requirements		Zones 1/2	Zones 3/4	Zones 5/6/7/8
U [W/m <sup>2</sup> K]	Exterior walls	0.479	0.705	0.705
	Exterior roofs	0.273	0.273	0.360
	Vertical glazing	3.410	3.970	6.810
SHGC	Vertical glazing	0.25	0.25	0.25



**Figure 3.** Brazilian bioclimatic zones. Reprinted with permission from ref. [18]. Copyright 2005 Associação Brasileira de Normas Técnicas (ABNT).

A medium/high occupation density is adopted according to the standard NBR 16401 [20], which considers a  $9.3 \text{ m}^2$  workplace and an equipment power density of  $16.2 \text{ W/m}^2$ . The light power density follows [8], which determines  $10.50 \text{ W/m}^2$  for offices,  $7.1 \text{ W/m}^2$  for corridors, and  $7.42 \text{ W/m}^2$  for the core (adopting the distribution of 30% for restrooms, 30% for stairs, 20% for technical areas and 20% for lift and technical shafts). The operation schedule used in the simulation follows the office building operation described in [21].

Figure 4 shows the diagram of the HVAC system considered for this study, following Appendix G of ASHRAE 90.1 [21]. It comprises an electric chiller with screw compressor and water condensation, a cooling tower with a two-speed axial fan, a primary chilled water circuit with constant flow and a secondary circuit with variable flow, interlocked chilled and condensing water pumps for each chiller, and air distribution by VAV boxes with electric coil for heating. To keep the primary loop water flow rate constant and the secondary loop flow rate variable it is necessary to install a bypass valve between the two loops to allow the difference in the flow between the secondary loop and the primary loop to recirculate in the primary loop.

A system with a capacity of less than 300TR was considered and an air renewal rate of  $27 \text{ m}^3/\text{person}/\text{hour}$  was adopted [22], as it is more restrictive than ASHRAE 62.1, [23] and [20]. The efficiencies of each piece of equipment used in the model (chiller, pumps, cooling towers, and fan-coils) are defined by [8].

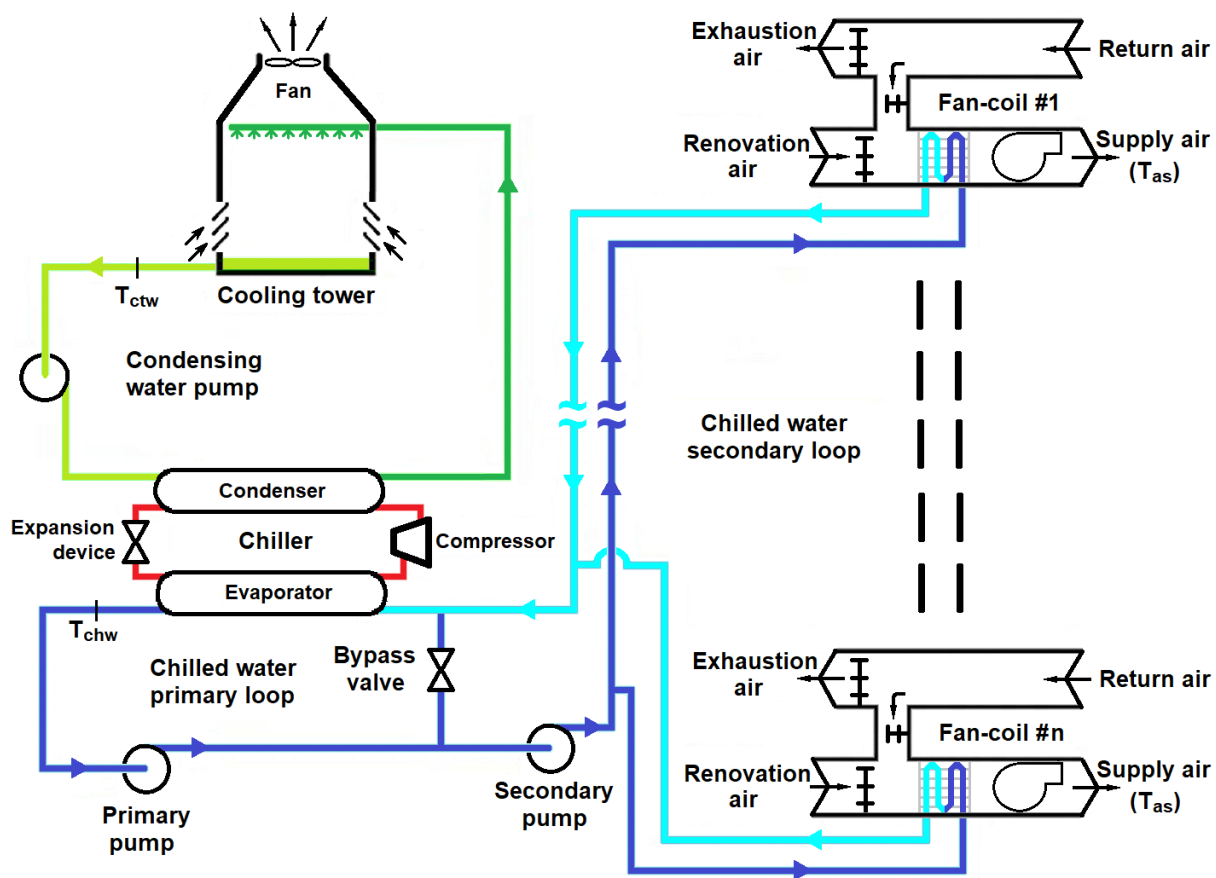


Figure 4. HVAC system diagram.

## 2.2. Modelling of Automation Control Strategies

The modelling follows the equations of the EnergyPlus™ documentation [24]. The Energy Management System (EMS) feature was used for implementing specific control strategies, which allows writing custom routines for EnergyPlus™ to describe the control algorithms.

EnergyPlus™ EMS has many objects, for example:

- EMS:Sensor to read some variable;
- EMS:Program to create a program that the user wants to run;
- EMS:Subroutine to create subroutines that can be called by the EMS:Program;
- EMS:ProgramCallingManager to specify when a given program should be executed;
- EMS:Actuator to actuate in the EnergyPlus™ as a controller.

EMS:Program was used to create a program that calculates at each time step the consumption of the equipment of HVAC for a temperature range ( $\pm 0.5$  °C) of the three temperatures studied. There was a program for each temperature ( $T_{chw}$ ,  $T_{as}$ ,  $T_{ctw}$ ) that calls a subroutine for each equipment consumption of the HVAC system. The temperature is varied in steps of 0.1 °C within the range considered, after which the temperature is adopted as the value that results in the lower HVAC energy consumption for the range.

For energy calculations, the EnergyPlus™ *Simulate Building System* was used. It is divided into 3 loops (air loop, plant loop, and condenser loop) according to Figure 5. Each loop has its own calculation, and for each loop calculation of the optimum temperature the temperatures of the other loops are kept fixed.

First, the optimal chilled water temperature ( $T_{chw}$ ) is calculated in plant loop with the other 2 temperatures fixed for the condition of the last timestep iteration. To avoid an oscillating effect in the chilled water loop, an operational range was used,  $T_{up}$  and  $T_{low}$ .

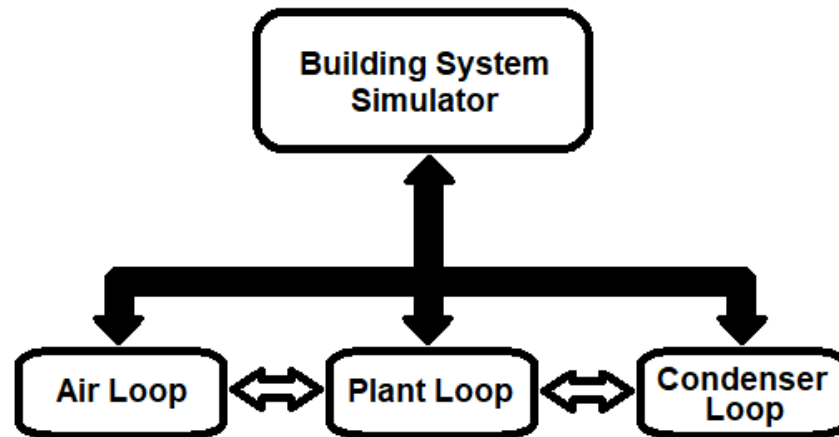


Figure 5. EnergyPlus™ Simulate Building System.

After that, the optimum  $T_{as}$  is calculated in air loop keeping  $T_{chw}$  fixed due to the limitation of the operational range of  $T_{chw}$ . The condenser loop does not affect the air loop, so  $T_{ctw}$  does not affect this calculation.

Lastly, the optimum  $T_{ctw}$  is calculated keeping the  $T_{chw}$  fixed with the optimum value previously calculated. The air loop does not affect the condenser loop, so  $T_{as}$  does not affect this calculation.

These calculations are executed at each iteration of the simulation, which is every 10 min. Since it is a small timestep, the variation in the new optimum temperatures is not great, normally less than 0.3 °C for each iteration.

#### 2.2.1. Effect of Chilled Water Outlet Temperature Variation ( $T_{chw}$ )

The increase in  $T_{chw}$  results in a reduction in the compression power of the chiller, but also leads to an increase in the chilled water flow that increases the pumping energy consumption. The impact of  $T_{chw}$  on chiller power consumption  $\dot{W}_{ch}$  is evaluated by the correction of the nominal performance curve  $\dot{W}_{ch} = f(\dot{Q}_{ref}, COP_{ref})$  by the functions CapFTemp (Equation (2)), EIRFTemp (Equation (3)), and EIRFPLR (Equation (4)).

$$\dot{W}_{ch} = (\dot{Q}_{ref}/COP_{ref}) \cdot CapFTemp \cdot EIRFT \cdot EIRPLR \quad (1)$$

with

$$CapFTemp = a_1 + b_1 T_{chw} + c_1 (T_{chw})^2 + d_1 T_{c,i} + e_1 (T_{c,i})^2 + f_1 T_{chw} T_{c,i} \quad (2)$$

$$EIRFTemp = a_2 + b_2 T_{chw} + c_2 (T_{chw})^2 + d_2 T_{c,2} + e_2 (T_{c,i})^2 + f_2 T_{chw} T_{c,i} \quad (3)$$

$$EIRFPLR = a_3 + b_3 PLR_{ch} + c_3 (PLR_{ch})^2 \quad (4)$$

$\dot{Q}_{ref}$  and  $COP_{ref}$  are, respectively, the nominal cooling capacity of the chiller and its coefficient of performance. CapFTemp is the cooling capacity factor as a function of operating temperature, EIRFTemp is the cooling power consumption as a function of operating temperature, and EIRFPLR is the cooling power consumption as a function of part-load ratio.  $T_{c,i}$  is the water temperature at the condenser inlet,  $PLR_{ch}$  is the part-load ratio (relation between the chiller required capacity and the capacity available in the chiller; the latter is affected by the CapFTemp curve), and the coefficients  $a_i$  to  $f_i$  are specific for each chiller.

In turn, the change in  $T_{chw}$  affects the power consumption of the pumps, as it causes a variation in the chilled water flow rate because  $T_{chw}$  changes the temperature difference in the plant loop, leading to a change in the water flow rate to meet the same thermal load. It alters the part-load performance of the pumps ( $PLR_p$ ), defined as the relationship between



the instantaneous water flow rate and the maximum water flow in the pump, affecting the power consumption of the pumps ( $\dot{W}_p$ ) according to Equation (5):

$$\dot{W}_p = \frac{\Delta p_p \cdot Q_{chw,max} (a_4 + b_4 PLR_p + c_4 PLR_p^2 + d_4 PLR_p^3)}{\eta_p \cdot \eta_{m,p}} \quad (5)$$

In Equation (5),  $\Delta p_p$  is the pump nominal head pressure of the pump, pressure,  $Q_{chw,max}$  is the maximum volumetric water flow rate of the chilled water pump,  $\eta_p$  and  $\eta_{m,p}$  are the pumping and motor efficiencies, and  $a_4$  to  $d_4$  are the specific coefficients for each pump.

A reduction in  $T_{chw}$  in a specific timestep implies that the chiller needs to remove not only the thermal load of the building, but also needs to remove the heat of the mass of water in the chilled water loop. This causes an overload of the chiller and increases its consumption, particularly at the beginning of working hours.

To avoid this overload in the chiller, the variation in  $T_{chw}$  was limited as a function of the actual chiller thermal load ( $CL_{actual}$ ), the reference thermal load ( $CL_{ref}$ ), and the minimum chilled water temperature obtained in the previous day ( $T_{chw,min}$ ) (at peak thermal load for the previous day)

However, the thermal load changes with timestep, and to avoid an oscillating effect in this temperature an operational range for this temperature was adopted between the upper ( $T_{up}$ ) and the lower limits ( $T_{low}$ ) of  $T_{chw}$ , given by Equations (6) and (7). In the second equation a safety factor (SF) is used. Therefore, when the temperature of the last timestep is between the upper and lower limits, this temperature is adopted as  $T_{chw}$ , avoiding oscillations.

$$T_{up} = 6.7 + (T_{min} - 6.7) \frac{CL_{ch} + CL_{actual}}{CL_{ch} + CL_{ref}} \quad (6)$$

$$T_{low} = 6.7 + (T_{min} - 6.7) \frac{CL_{ch} + SF \cdot CL_{actual}}{CL_{ch} + CL_{ref}} \quad (7)$$

Before the peak, the chiller thermal load ( $CL_{ch}$ ) in Equations (6) and (7) is adopted as  $CL_{ref}$ , the thermal load of the same period of the previous day. After the peak thermal load and before the end of the business hours (18 h),  $T_{chw}$  is adopted as the minimum temperature calculated in the actual day before 8 h, and it is not necessary to calculate the limits. After the end of business hours, the peak thermal load of the actual day is adopted as  $CL_{ref}$ . For the security factor, the adopted values are 1.5 before 8 h, 1.3 between 8 h and 11 h, 1.2 between 11 h and the peak thermal load, and the value of 1.1 after the end of the business hours (18 h). Note that  $T_{chw}$  should not exceed 10 °C to avoid compromising the air temperature outlet in the fan-coil (12.8 °C).

### 2.2.2. Effect of Changing the Supplied Air Temperature ( $T_{as}$ )

Increase in  $T_{as}$  implies an increase in the air supply flow rate to reach the same thermal load, which increases the fan power consumption in the fan-coil. However, increasing  $T_{as}$  allows the increase in  $T_{chw}$ , reducing the chiller consumption. The change in  $T_{as}$  alters the fan consumption by the variation in the enthalpy in the cooling coil outlet of the fan-coil ( $h_{out,air}$ ), which in turn changes the air supply mass flow ( $\dot{m}_{air}$ ) required to meet the thermal load, according to Equation (8).

$$\dot{m}_{air} = \dot{Q}_{coil} / (h_{in,air} - h_{out,air}) \quad (8)$$

where  $\dot{Q}_{coil}$  is the rate of heat transfer in the cooling coil and  $h_{in,air}$  is the enthalpy of supplied air at the cooling coil inlet, which is a function of the enthalpy of the supplied air outlet in the mixing box and the dissipated heat for the fan in the air loop.

With the change in the air mass flow, the value of the fan-coil flow fraction ( $f_{fc}$ ) is affected as regards the maximum mass flow in the fan-coil; that affects the fan's consumption ( $\dot{W}_{fc}$ ), according to Equation (9). However, these changes the dissipated heats for the fan in the air loop, and consequently affect the enthalpy in the cooling coil inlet, which affects Equation (8). Hence, the solution of the equations will be solved interactively.

$$\dot{W}_{fc} = \dot{W}_{nom,fc} \left( a_5 + b_5 f_{fc} + c_5 f_{fc}^2 + d_5 f_{fc}^3 + e_5 f_{fc}^4 \right) \quad (9)$$

where  $\dot{W}_{nom,fc}$  is the fan power at nominal conditions and  $a_5$  to  $e_5$  are the coefficients for a given equipment.

The impact in the chilled water loop is related to the possibility of increasing  $T_{chw}$ , which is attached to  $T_{as}$  for Equation (10). As presented before, when  $T_{chw}$  changes, the flow of the chilled water also changes. Therefore, the optimum  $T_{as}$  is obtained considering the change in the fans, chiller and pump consumptions.

$$T_{chw} = 6.7 + (T_{as} - 12.8) \quad (10)$$

According to [22,25], the maximum relative humidity (when considering the setpoint of 24 °C) is 65%. Therefore, the lower  $T_{as}$  limit is 15 °C, for which the maximum relative humidity is approximately 60%.

### 2.2.3. Effect of the Variation in Cooling Tower Outlet Water Temperature ( $T_{ctw}$ )

The reduction in  $T_{ctw}$  implies a reduction in the chiller compression power; however, this also implies a higher consumption of the fans in the cooling tower. The impact on the cooling tower is reflected in the change in condensing water temperature in the condenser outlet (cooling tower inlet), which affects the fraction of time the cooling tower must operate in high-fans speed (100% of the capacity) (Equation (11)), in low-fans speed (50% of the capacity) (Equation (12)), or at free convection; that is, when the fans are turned off (for such a condition, 10% of the capacity were adopted).

$$F_{100} = \frac{T_{ctw,in} - T_{ctw,out,low}}{T_{ctw,out,high} - T_{ctw,out,low}} \quad (11)$$

$$F_{50} = \frac{T_{ctw,in} - T_{ctw,out,off}}{T_{ctw,out,low} - T_{ctw,out,off}} \quad (12)$$

where  $T_{ctw,out,high}$  is the outlet temperature of the cooling tower if the fans are working with 100% capacity,  $T_{ctw,out,low}$  is the outlet temperature if the fans are working with 50% capacity, and  $T_{ctw,out,off}$  is the outlet temperature if the cooling tower is working in free convection. With Equations (11) and (12) it is possible to calculate the average power of the cooling tower as a function of the condenser temperature, Equation (13):

$$\dot{W}_{ct,avg} = \begin{cases} F_{100} \dot{W}_{ct,high} + (1 - F_{100}) \dot{W}_{ct,low} \\ F_{50} \dot{W}_{ct,low} \\ 0 \end{cases} \quad (13)$$

where  $\dot{W}_{ct,avg}$  is the average power consumption of the cooling tower fans in a specific time step in the simulation;  $\dot{W}_{ct,high}$  is the nominal cooling tower power at full capacity, and  $\dot{W}_{ct,low}$  is the consumption when the cooling tower works at 50% capacity.

As mentioned before, the  $T_{chw}$  effect on chiller consumption can be evaluated by Equations (2)–(4). Since changes in chiller consumption change the temperature at the condenser outlet, it is necessary to solve the problem interactively to obtain the  $T_{chw}/T_{ctw}$  pair that optimizes the HVAC consumption.



### 3. Results

The results of the control strategies developed in this study were compared with two reference models. The first follows RTQ-C [7], which does not define any kind of control for the three temperatures. In this model, the temperatures were kept fixed at design conditions. The second model follows ASHRAE 90.1 [8], which defines that  $T_{chw}$  and  $T_{ctw}$  should be controlled as a function of the weather conditions but does not establish any control of  $T_{as}$  for the Brazilian weather conditions.

The results for the  $T_{chw}$  isolated control (Figure 6) show an annual reduction in relation to the base model that varies between  $-3.59\%$  and  $-6.76\%$ ; in relation to the ASHRAE model (considering only the  $T_{chw}$  control), the annual reduction is between  $-2.43\%$  and  $-3.83\%$ .

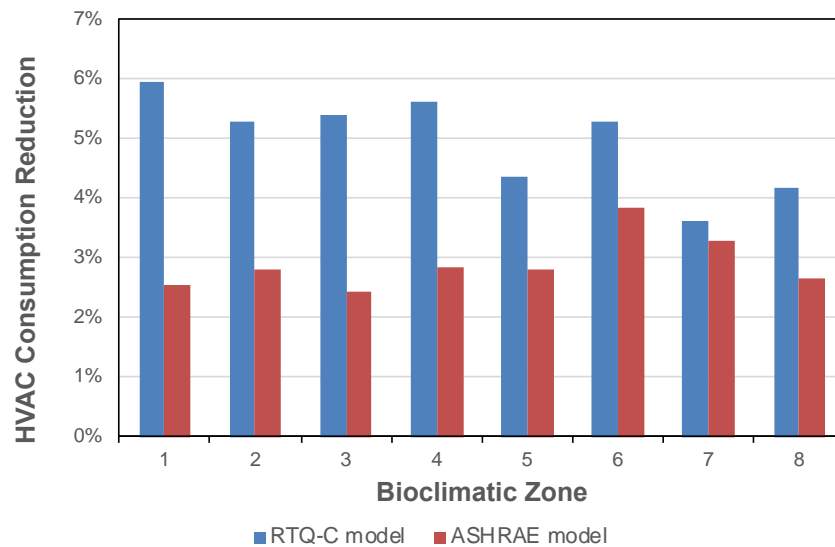


**Figure 6.** HVAC reduction for  $T_{chw}$  isolated optimisation control.

Regarding the isolated  $T_{ctw}$  control (Figure 7), there is a more significant reduction in relation to the RTQ-C model (ranging  $-1.77\%$  to  $-11.58\%$ ). Compared to the ASHRAE model (considering only the  $T_{ctw}$  control), the reductions vary between  $-0.23\%$  and  $-2.42\%$ . Note that the minimum  $T_{ctw}$  that can be obtained depends directly on the wet bulb external temperature; hence, the weather limits the gains that can be obtained.

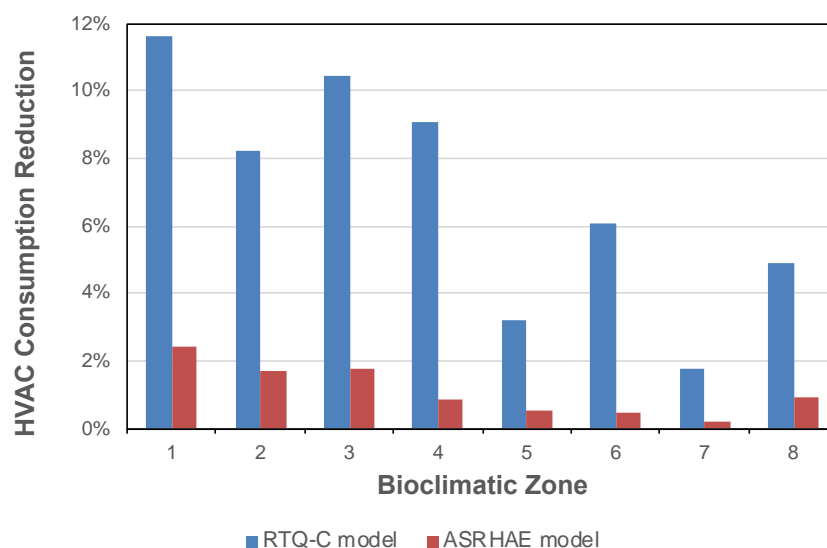


**Figure 7.** HVAC reduction for  $T_{ctw}$  isolated optimisation control.

Taking into account the result for the isolated  $T_{as}$  control (Figure 8), only zones 1 to 3 have a reduction in energy consumption in relation to the RTQ-C model, with the highest reduction ( $-6.26\%$ ) for cold weather (zone 1) and the lowest for zone 3 ( $-2.04\%$ ). For the other zones (4 to 8), there is no significant reduction in consumption, which indicates that the gains may be related to colder weather.

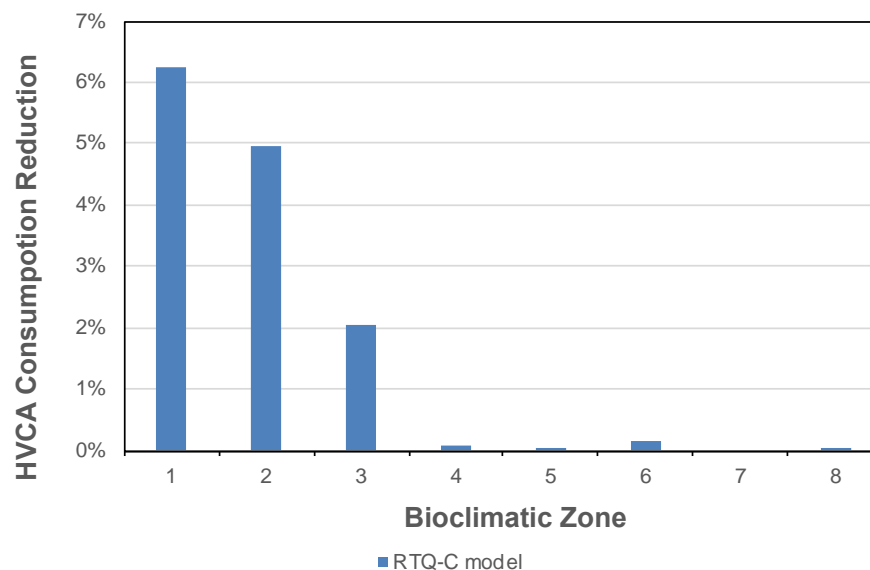


Figure 8. HVAC Reduction for  $T_{as}$  isolated optimization control.

Comparing the three isolated controls, it can be noted that  $T_{chw}$  control has the most homogeneous behaviour for the different weather conditions when compared to the other two isolated controls.

When two controls are integrated (Figures 9–11), there are greater reductions, as pointed out in the literature [3,10–17], which shows that integration is important and must be considered in control strategies. However, note that the reduction in integration is not the sum of the isolated reduction because the controls are interrelated.

Finally, when analyzing the reduction in consumption with the three integrated models (Figure 12), the results vary in relation to the RTQ-C model between  $-5.03\%$  and  $-19.68\%$ , and in relation to the ASHRAE model between  $-3.22\%$  and  $-8.21\%$ . The highest reductions are for zones 1 to 3, due to the interaction with the  $T_{as}$  control.

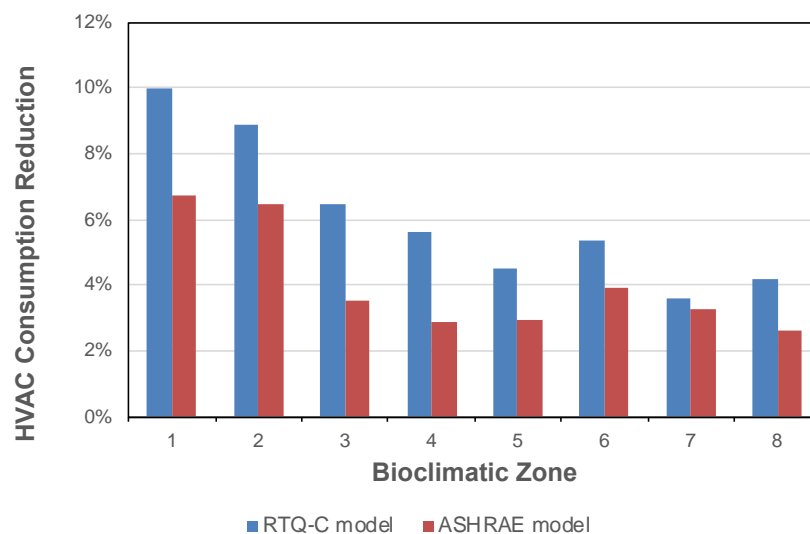


Figure 9. HVAC reduction for  $T_{ch}/T_{as}$  integrated optimisation control.

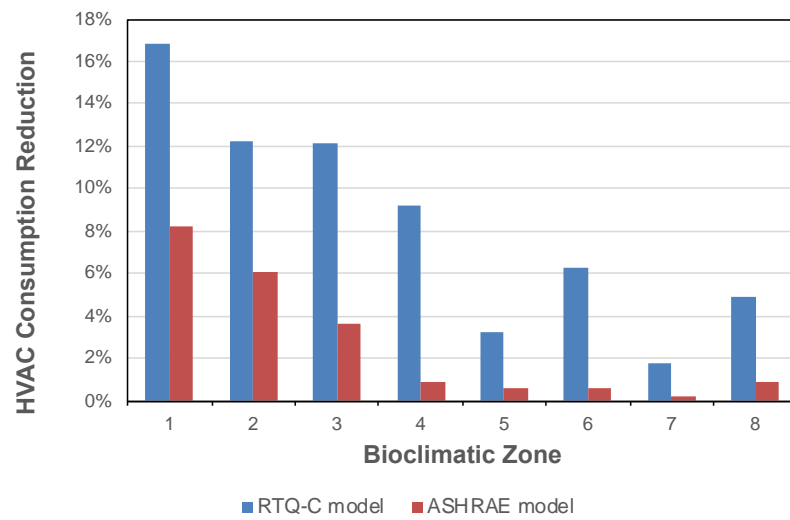


Figure 10. HVAC Reduction for  $T_{ctw}/T_{as}$  integrated optimization control.

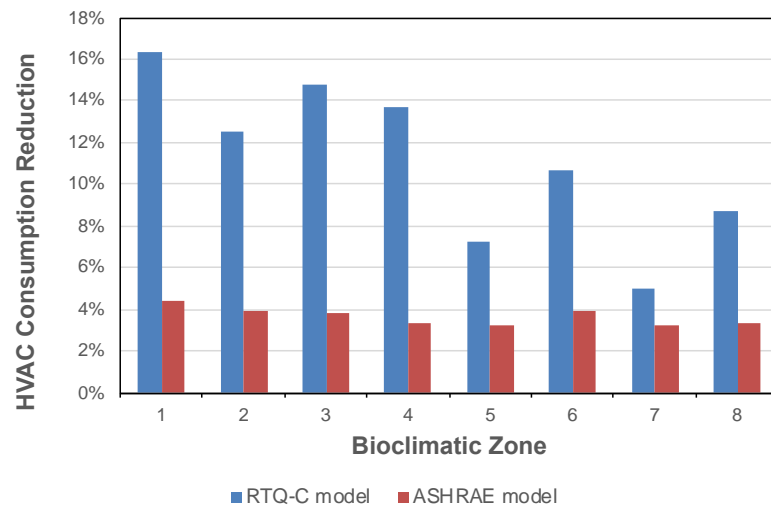


Figure 11. HVAC Reduction for  $T_{ch}/T_{ctw}$  integrated optimization control.

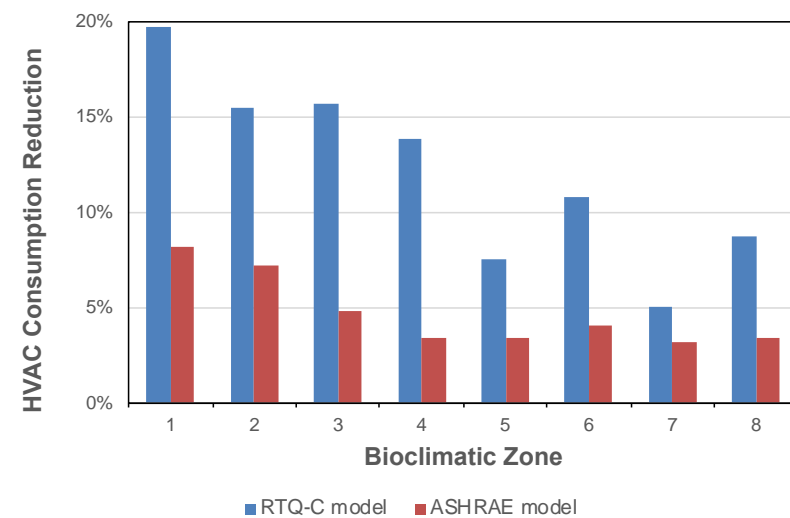


Figure 12. HVAC Reduction for the three integrated optimization controls.

#### 4. Discussion

The results for the chilled water temperature control showed reductions in relation to the RTQ-C model that varied between 3.59% and 6.76%, and in relation to the AHSRAE model the reductions vary between 2.43% and 3.83%.

Note that  $T_{\text{chw}}$  control presented a more homogeneous behaviour between the different climatic conditions when compared to the other controls considered in this work. When analyzing the results of controlling the air supply temperature, only bioclimatic zones 1 to 3 showed reductions in consumption, with the largest reductions for the coldest climate (6.26%) and the smallest for the bioclimatic zone 3 (2.04%). For the other bioclimatic zones (4 to 8), there were no significant reductions in consumption. It is important to highlight that even bringing gains for climates with colder temperatures (or mild for the conditions in the USA and Europe), the ASHRAE 90.1 standard does not present a control for this temperature, precisely because it considers these climates mild and not cold.

Analyzing the results from the condensing temperature control in relation to the RTQ-C model, the gains obtained showed a more significant variation (from 1.77% to 11.58%), showing the highest gains among the three controls isolated for bioclimatic zones 1 to 4. For zones 5, 6 and 8 the gains were smaller, being close to the gains obtained with the chilled water control, and only in zone 7 this control showed lower gains than the chilled water temperature control. Compared to the ASHRAE model, the reductions range from 0.23% (also in zone 7) to 2.42%.

The RTQ-C model has much lower consumption in the cooling tower than the other models (from 2 to 3 times lower), as this equipment operates most of the year in free flow or with only 1 of the speeds due to the fixed control with a high value. However, this overloads the chiller, which shows that it would be important to control this variable, since the chiller is the element of the HVAC system that consumes the most energy.

Increasing the temperature of the condensation water directly affects two parameters of the air conditioning system: the first is the chiller consumption when the condensing temperature decreases, and the second is the cooling tower consumption when the air flow increases.

As we integrate one or more controls the reductions become greater, showing that this integration is important and must be considered. However, note that the reduction obtained with the integration is lower than the sum of the isolated reductions, as the controls end up interfering with each other.

For example, in a hypothetical situation in which it was possible to use the three controls without mutual interference, the reductions in relation to the ASHRAE model for bioclimatic zone 1 would have isolated gains of 2.52%, 6.26%, and 2.42%, respectively, for the control of chilled water, supplied air, and condensation water temperature (totalling 11.20%). In the same situation, the reduction in the integrated model is 8.21%, lower than the sum of the isolated models (11.2%).

Analyzing the reductions in the three integrated controls in relation to the RTQ-C model, the results vary from 5.03% (zone 7) to 19.68% (zone 1), and for the ASHRAE model the results vary from 3.22% (zone 7) to 8.21% (zone 1). Gains are greater for bioclimatic zones 1, 2 and 3, as these zones show gains with control of the supplied air temperature, which do not occur for the others.

Observe that the control that takes into account the external temperatures proposed by ASHRAE presents better results than the RTQ-C model, and that the model proposed herein, when also considering the variation in the thermal load, brings additional gains to the model currently used as a reference for the market; this demonstrates the importance of making a more precise control for each climatic condition, not only in function of the external conditions but also of the thermal load of the building.

One last important aspect to highlight in relation to the results is that its implementation has a basically negligible cost in terms of return on investment, as it basically involves the man-hour cost for reprogramming the control logic of existing systems and eventually a readjustment/repositioning of some sensors and controls.

**Author Contributions:** Conceptualization, and methodology, J.D.-V. and F.A.S.F.; model implementation and simulations, J.D.-V.; formal analysis, J.D.-V. and F.A.S.F.; writing—original draft preparation, J.D.-V. and F.A.S.F.; writing—review and editing, F.A.S.F.; supervision, F.A.S.F. All authors have read and agreed to the published version of the manuscript.

**Funding:** This research received no external funding.

**Data Availability Statement:** The research data is available upon request.

**Conflicts of Interest:** The authors declare no conflict of interest.

## References

1. Li, N.; Yang, Z.; Becerik-Gerber, B.; Tang, C.; Chen, N. Why is the reliability of building simulation limited as a tool for evaluating energy conservation measures? *Appl. Energy* **2015**, *159*, 196–205. [CrossRef]
2. Vakiloroyaya, V.; Samali, B.; Fakhar, A.; Pishghadam, K. A review of different strategies for HVAC energy saving. *Energy Conserv. Manag.* **2014**, *77*, 738–754. [CrossRef]
3. Li, X.; Li, Y.; Seem, J.E.; Li, P. Dynamic modeling and self-optimizing operation of chilled water system using extremum seeking control. *Energy Build.* **2013**, *58*, 172–182. [CrossRef]
4. EPE. Brazilian Energy Balance—Year 2020. Available online: <https://ben.epe.gov.br/> (accessed on 6 September 2022).
5. Gruder, M.; Trüschel, A.; Dalenbäck, J.O. Alternative strategies for supply air temperature control in office building. *Energy Build.* **2014**, *82*, 406–415. [CrossRef]
6. ELETROBRAS. *Pesquisa de Posse de Equipamentos e Hábitos de Uso, Ano Base 2005: Classe Residencial Relatório Brasil—Sumário Executivo*; ELETROBRAS: Rio de Janeiro, Brazil, 2009; Available online: <http://www.procelinfo.com.br> (accessed on 6 September 2022).
7. PBEE. *RTQ-C Application Manual—Commercial, Services and Public—Version 4.1*; PBEE: Rio de Janeiro, Brazil, 2017; (In Portuguese). Available online: <https://www.pbenedifica.com.br/> (accessed on 6 September 2022).
8. *Standard 90.1*; Energy Standard for Building Except Low-Rise Residential Building. ASHRAE: Atlanta, GA, USA, 2010.
9. Argüello-Serrano, B.; Vélez-Reyes, M. Nonlinear Control of a Heating, Ventilation, and Air Conditioning System with Thermal Load Estimation. *IEEE Trans. Control. Syst. Technol.* **1999**, *7*, 56–63. [CrossRef]
10. Ahn, B.C.; Mitchell, J.W. Optimal control development for chilled water plants using a quadratic representation. *Energy Build.* **2001**, *33*, 371–378. [CrossRef]
11. Albieri, M.; Beghi, A.; Bodo, C.; Cecchinato, L. Advanced control for single compressor chiller units. *Int. J. Refrig.* **2009**, *32*, 1068–1076. [CrossRef]
12. Wang, G.; Song, L. Air handling unit supply air temperature optimal control during economizer cycles. *Energy Build.* **2012**, *49*, 310–316. [CrossRef]
13. Ke, Y.P.; Mumma, S.A. Optimized supply-air temperature (SAT) in variable-air-volume (VAV) system. *Energy* **1997**, *22*, 601–614. [CrossRef]
14. Braun, J.E.; Diderrich, G.T. Near-optimal control of cooling towers for chilled-water system. *ASHRAE Trans.* **1990**, *96*, 806–816.
15. Liu, C.W.; Chuah, Y.K. A study on an optimal approach temperature control strategy of condensing water temperature for energy saving. *Int. J. Refrig.* **2011**, *34*, 816–823. [CrossRef]
16. Parameshwaran, R.; Karunakaran, R.; Iniyan, S.; Samuel, A.A. Optimization of energy conservation potential for VAV air conditioning system using fuzzy based genetic algorithm. *Int. J. Mech. Aerosp. Mechatron. Manuf. Eng.* **2008**, *2*, 223–230. [CrossRef]
17. Lee, K.P.; Cheng, T.A. A simulation-optimization approach for energy efficiency of chilled water system. *Energy Build.* **2012**, *54*, 290–296. [CrossRef]
18. *Standard NBR 15220*; Thermal Performance in Buildings—Part 3: Brazilian Bioclimatic Zones and Building Guidelines for Low-cost Houses. ABNT: Rio de Janeiro, Brazil, 2005. (In Portuguese)
19. DOE. *EnergyPlus™—Weather Data by Region*; DOE: Washington, DC, USA, 2018; Available online: <https://energyplus.net/weather> (accessed on 15 July 2018).
20. *Standard NBR 16401*; Central and Unitary Air Conditioning Systems. ABNT: Rio de Janeiro, Brazil, 2008. (In Portuguese)
21. *Standard 90.1*; User’s Manual: Energy Standard for Building Except Low-Rise Residential Building. ASHRAE: Atlanta, GA, USA, 2007.
22. ANVISA. Resolution RE/ANVISA 176/2000. Available online: <http://www.anvisa.gov.br/> (accessed on 6 September 2022).
23. *Standard 62.1*; Ventilation for Acceptable Indoor Air Quality. ASHRAE: Atlanta, GA, USA, 2007.
24. DOE. *EnergyPlus™ Version 8.1 Documentation—Engineering Reference*; DOE: Washington, DC, USA, 2013; Available online: <https://energyplus.net/documentation> (accessed on 15 July 2018).
25. *Standard 55*; Thermal Environmental Conditions for Human Occupancy. ASHRAE: Atlanta, GA, USA, 2017.

**Disclaimer/Publisher’s Note:** The statements, opinions and data contained in all publications are solely those of the individual author(s) and contributor(s) and not of MDPI and/or the editor(s). MDPI and/or the editor(s) disclaim responsibility for any injury to people or property resulting from any ideas, methods, instructions or products referred to in the content.